Micromodular Implants to Provide Electrical Stimulation of Paralyzed Muscles and Limbs

Tracy Cameron,* *Member, IEEE*, Gerald E. Loeb, Raymond A. Peck, Joseph H. Schulman, *Life Member, IEEE*, Primoz Strojnik, and Philip R. Troyk, *Senior Member, IEEE*

***Abstract*— We describe the design, fabrication, and output capabilities of a microminiature electrical stimulator that can be injected in or near nerves and muscles. Each single-channel microstimulator consists of a cylindrical glass capsule with hermetically sealed electrodes in either end (2-mm diameter × 13-mm overall length). Power and digital control data can be transmitted to multiple implants (256 unique addresses) via a 2-MHz RF field created by an external AM oscillator and inductive coil. *In vitro* testing demonstrated accurate control of output pulsewidth (3–258 μs in 1-μs steps) and current (0–30 mA in two linear ranges of 16 steps each, up to 8.5 V available compliance voltage). Microstimulators were used successfully for chronic stimulation in hindlimb muscles of cats. Design and fabrication issues affecting yield and reliability of the packaging and electronics are discussed.**

***Index Terms*—FES, FNS, muscle, paralysis, stimulator, TES.**

I. Introduction

THERAPEUTIC electrical stimulation (TES) can strengthen muscles paralyzed from upper motor injury or disease [1], [2] or those that have atrophied from inactivity following surgery or trauma [3]–[5]. Functional neuromuscular stimulation (FNS) has provided individuals with the ability to initiate movements that are of functional value, such as the restoration of limited grasping functions after cervical spinal cord injury [6]–[9], and the restoration of ambulation by FNS alone [10], [11] or in combination with orthotics [12]–[14]. FNS has also been used to improve ventilation by stimulation of the phrenic nerve [15], [16], improve bladder, bowel, and sexual function by stimulation of the sacral anterior nerve roots [17]–[20], and reduce spasticity [21], [22].

Two main interface techniques have been used in the application of FNS to paralyzed muscle. The first involves surgically implanting electrodes directly in or on muscles and nerves. Control of these types of electrodes has been accomplished by using fully implanted multichannel systems that require long wire leads to connect remote electrodes to a central controller. The intramuscular electrodes typically used in these systems are subject to mechanical failure [23], while the tunneling of the lead wires can cause tissue damage [24]. A major disadvantage of these systems is the absence of redundancy in the event of a system failure [24]. Percutaneous wires implanted into muscles have also been used, but pose unacceptable problems of cosmesis, maintenance, and infection [25]–[27]. The second strategy has been to apply surface electrodes to the skin over the muscles of interest, but the recruitment of individual muscles is not sufficiently selective for applications requiring fine control of motion. These electrodes can also be difficult to don and maintain, and may produce skin irritation and unpleasant sensations related to activation of cutaneous nerves [28]–[30]. Several groups of researchers have attempted to solve some of these problems by designing single-channel implantable stimulators. These miniaturized stimulators can be located at or near their individual targets [31], [32]. These devices, though fairly small, were of limited use because they did not provide the stimulus control and multichannel addressability needed for most motor tasks. The device developed by Waters *et al.* [31] was designed solely to correct foot drop, while the device designed by Strojnik *et al.* [32] required a separate external controller for each implant.

We are developing implantable electronic devices that can be used in a variety of combinations to stimulate individual nerves and muscles. These devices eliminate the donning and reliability problems of surface and percutaneous electrodes, and do not require long leads between the electrodes and the controller because the receiving and stimulating circuitry are contained within each unit. Their small size allows injection directly into the desired muscles through a hypodermic needle, providing for unlimited combination of a multiple of individually selective channels. The enabling technology and specifications of the microstimulator have been described previously [33]; we here describe the actual fabrication and *in vitro* test results of the functioning device.

II. Methods

A. Design, Fabrication, and Control Specifications

1) Specifications:

a) Size: 2-mm diameter, 13-mm length.

b) Packaging: hermetically sealed glass encapsulation.

Manuscript received October 13, 1995; revised May 5, 1997. This work was supported by the Ontario Rehabilitation Technology Consortium, Canadian Neuroscience Network of Centres of Excellence, and the U.S. National Institutes of Health, under Research Contracts N01-NS-2-2322 and N01-NS-5-2325. *Asterisk indicates corresponding author.*

*T. Cameron was with Queen's University, Biomedical Engineering Unit, Abramsky Hall, Kingston, Ont. K7L 3N6 Canada (e-mail: tracy@biomed.queensu.ca.). She is now with the Division of Neuroscience, University of Alberta, Edmonton, Alta. T6G 252 Canada.

G. E. Loeb and R. A. Peck are with Queen's University, Biomedical Engineering Unit, Kingston, Ont. K7L 3N6 Canada.

J. H. Schulman and P. Strojnik are with the A. E. Mann Foundation for Scientific Research, Sylmar, CA 91342 USA.

P. R. Troyk is with the Illinois Institute for Technology, Chicago, IL 60616 USA.

Publisher Item Identifier S 0018-9294(97)06105-3.

Fig. 1. Microstimulator, from left: anodized Tantalum (Ta)-slug, hermetic seal to glass bead and glass capillary walls, Ta stem welded to gold plated metal shim, integrated circuit (IC) chip with Au wirebonds to copper (Cu) coil, Ag-epoxy junctions to Cu coil windings over hollow ferrite core, Ag-epoxy connection to iridium (Ir) ball sealed to glass capillary wall, activated Ir surface.

TABLE I
LIST OF THE REQUIREMENTS FOR MICROMINIATURE STIMULATOR

Requirements	Implementation
minimal surgery	small size allows injection into muscle through hypodermic needle
custom configuration	multiple single-channel stimulators can be combined in an unlimited manner
avoid lead breakage	wireless transmission of data and power
long life	hermetic package, no batteries
safe	capacitive charge storage, charge-balanced output stimulation
precise	digitally controlled stimulating-current amplitude and duration
biocompatibility	only materials known to be biocompatible are used for electrodes and encapsulation
stable tissue interface	package designed for tissue fixation without progressive encapsulation

TABLE II
LIST OF THE VARIOUS COMPONENTS AND THEIR SPECIFICATIONS USED IN THE MANUFACTURE OF THE MICROSTIMULATOR

Part Name	Specification
Glass Capillary	N51A borosilicate, 0.079" OD ±0.001"
Glass Bead	0.015"ID, 0.065" OD. 0.04" thickness
Glass Washer[1]	0.015"ID, 0.065" OD. 0.01" thickness
Ferrite Top	0.025" radius, 0.16" core length
Ferrite Bottom	0.025" radius, 0.24" core length
Tantalum Slug[2]	0.046" diameter, 0.039" thickness
Iridium Ball[3]	0.065" diameter
Gold Plated Metal Shim	0.18" length, 0.042" width, 0.004" height
Gold Plated Wire Feedthrough	0.008" OD, 0.2" long
Integrated Circuit Chip	3 μm, double poly, c-mos, p-well
Diode	THD 9064
Copper Coil	0.001" diameter insulated wire

[1] Kimbel borosilicate glass type N51A, formed by Friedrich & Dimmock, Millvile, NJ.
[2] AVX Tantalum Corp. Biddeford, ME.
[3] Melted on end of 0.01″-diameter wire from Englehard Industries, Aurora, Ont., Canada.

c) Power: inductive coupling from an external coil (2 MHz).
d) Physical range: anywhere within a cylindrical coil or one radius from the face of a flat coil.
e) Number of unique addresses: 256
f) Pulse width control: 3–258 μs, 1-μs steps.
g) Pulse amplitude control: 0.2–30 mA in two ranges of 15 linear steps each (0.2 and 2 mA, respectively).
h) Pulse waveform: charge-balanced.
i) Waveform options: two recharge current settings, 20 or 200 μA; two pulse shapes, square or exponential tail.

2) Package Design Considerations: The main distinguishing feature of microstimulator-based applications is that multiple stimulators can be implanted with minimal surgery. The size and shape of the device was restricted to a cylindrical capsule to permit injection through a 12-gauge hypodermic needle (Fig. 1). A second feature of the device concerns the control of multiple implants. Each device must contain circuitry that is uniquely addressable and capable of delivering a variety of pulse durations and intensities. A third feature is long life, which requires that internal components of the stimulator be electronically isolated from the body fluids, and power and data be transmitted through RF coupling (Tables I and II).

Biocompatible borosilicate glass was used to encapsulate the internal components hermetically while adhering to the constraints on package size and electromagnetic transmission. Sintered tantalum (Ta) was used as one electrode material because it is able to act as a "capacitor-electrode" with respect to body fluids [34]. In this application, the stimulus charge must be accumulated between pulses and stored on the electrode material itself because the limited size of the device does not allow for the inclusion of an internal storage capacitor. Iridium (Ir) was chosen as the other electrode material because of its nonpolarizing, low-impedance interface when activated. This combination of tantalum and iridium has been found to perform well during extensive electrochemical testing [33].

Ir activation was required in order to increase charge storage and lower the interface impedance. However, Ir activation could not survive the heat required to fuse the Ir ball to the glass capillary. Similarly, sintered Ta is somewhat fragile and can be damaged or contaminated during the assembly process. Electrochemical conditioning of both the Ir and Ta electrodes were, therefore, carried out after the capsule was sealed as described previously [33].

3) Tantalum Electrode: Loosely packed tantalum powder was sintered on the end of a solid Ta wire (0.25-mm diameter) to form a porous tantalum cylinder (slug) many times increasing its available surface area (geometric surface area 9.60 mm^2). The anodization of tantalum forms a dielectric of tantalum pentoxide whose thickness is proportional to the anodization voltage (2 nm per V) [34]. After assembly into the microstimulator, the Ta electrode was anodized by applying a current of 0.1 mA with a compliance of 37 V and holding for 1 h longer than required to reach the compliance limit. The anodization current was applied by probing the iridium electrode and passing the current through the internal circuitry

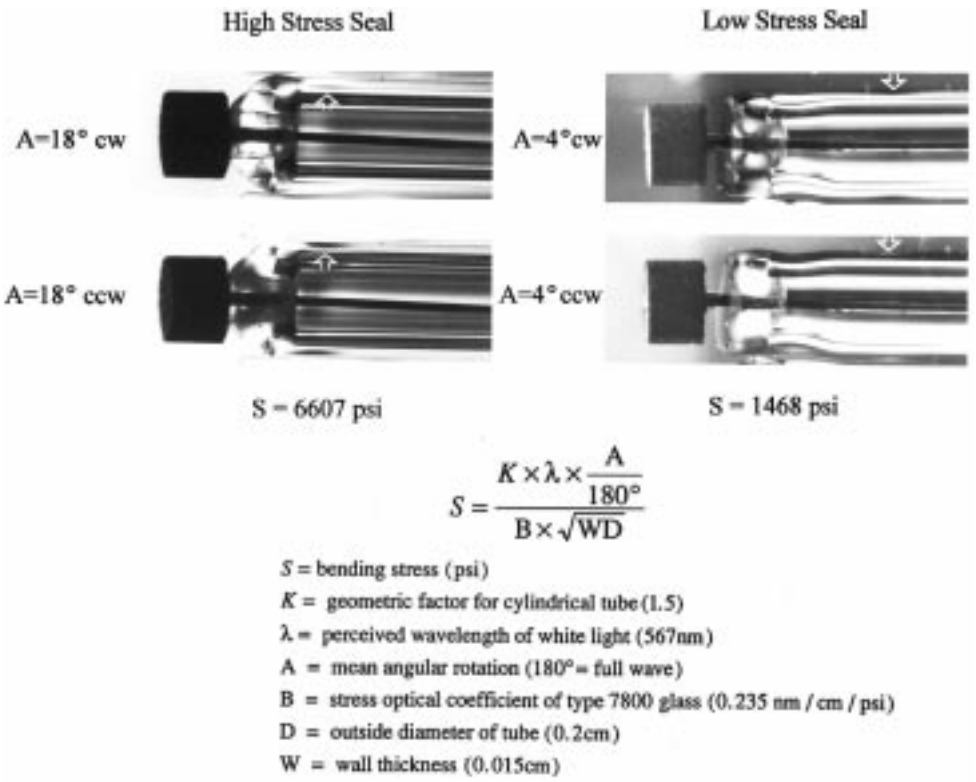

Fig. 2. Photograph showing regions of high and low stress (arrows) determined by observing the devices under polarized light and examining for nulls (shown by dark regions). Quantitative results for the stresses were made by applying the various values to the formula shown below the photograph. Stress measurements below 2000 lb/in^2 (140 kg/cm^2) are considered desirable for such glass-to-metal seals.

and out the tantalum electrode, which was immersed in 0.1% phosphoric acid solution.

4) Iridium Electrode: During operation of the microstimulator, the Ir electrode is polarized cathodically with respect to tantalum. Iridium is an excellent electrode material, as it can be electrochemically activated using cyclic voltammetry [35], forming a multilayer film of oxide. Each Ir atom in the oxide can accept or donate one electron by shifting valence as shown below. This provides as much as a 100-fold increase over the charge capacity of surface double-layer charging [36]

$$\mathrm{Ir}^{+3}(\mathrm{OH})_3 + \mathrm{H_2O} \Leftrightarrow \mathrm{Ir}^{+4}(\mathrm{OH})_4 + \mathrm{H}^+ + e^-$$
$$\mathrm{Ir}^{+3}(\mathrm{OH})_3 + \mathrm{OH}^- \Leftrightarrow \mathrm{Ir}^{+4}(\mathrm{OH})_4 + e^-.$$

Activation was accomplished by touching an iridium probe wire to the electrode surface. Although this procedure results in an area of incomplete activation at the contact point between probe wire and electrode surface, the electrochemical properties of incomplete Ir coatings are known to be dominated by the activated region [35]. Iridium was activated by repetitive cycling at 500 mV/s between -0.64 V and $+0.86$ V versus saturated calomel electrode in phosphate buffered saline (PBS). The charge capacity after 1 h of activation increased from a preactivation capacity of 1.2 mC/cm^2 to 15.6 mC/cm^2.

5) Hermetic Seals: The electronic circuitry was hermetically sealed in Kimbel N51A borosilicate glass. Borosilicate glass is biocompatible [37] and stable at neutral pH, which enables it to maintain hermeticity for extended periods of time. Another important reason for using glass is that it can be melted to form seals to other oxide surfaces such as those on most metals. Three such seals are needed in the fabrication of the microstimulator; glass-to-Ta, glass-to-Ir, and glass-to-glass. Similar seals in military diodes and magnetic reed relays are usually tested to 1×10^{-8} cm^{3}s^{-1} atmosphere^{-1} helium. Our glass-to-metal seals must pass helium leak tests at the limit of practical detection of 1×10^{-10} cm^{3}s^{-1} atmosphere^{-1}. Even so, the small volume of the microstimulator makes it extremely sensitive to any water that may be trapped in the package at the time of sealing or that leaks into the package subsequently. The water vapor that would pass through a leak just below our sensitivity limit would reach 100% humidity in about 200 days. We can greatly increase this time by introducing a small (1 mm^3) crystal of a hygroscopic salt such as cobalt chloride. This same leak would then require over 9000 years before saturation would occur.

Stresses created during sealing can lead to cracks, particularly at scratches or abrasions on the glass, where stress leads to the propagation of cracks in the presence of a polar liquid such as water [38]. Quantitative analysis of the stress in low- and high-stress seals is shown in Fig. 2. Stress in glass can be evaluated as a function of optical retardation. Retardation is measured by rotating crossed polarizing filters until all transmitted light in the local region is extinguished. A quarter-wave filter was inserted into a polarimeter converting the light to a monochromatic state. By rotating the cross polaroid either clockwise (CW) or counterclockwise (CCW), nulls are attained in regions of stress. These regions are marked by the arrows in Fig. 2 [38] and are barely visible in the low-stress seals. The mean angular rotation and the cylindrical geometrical factors

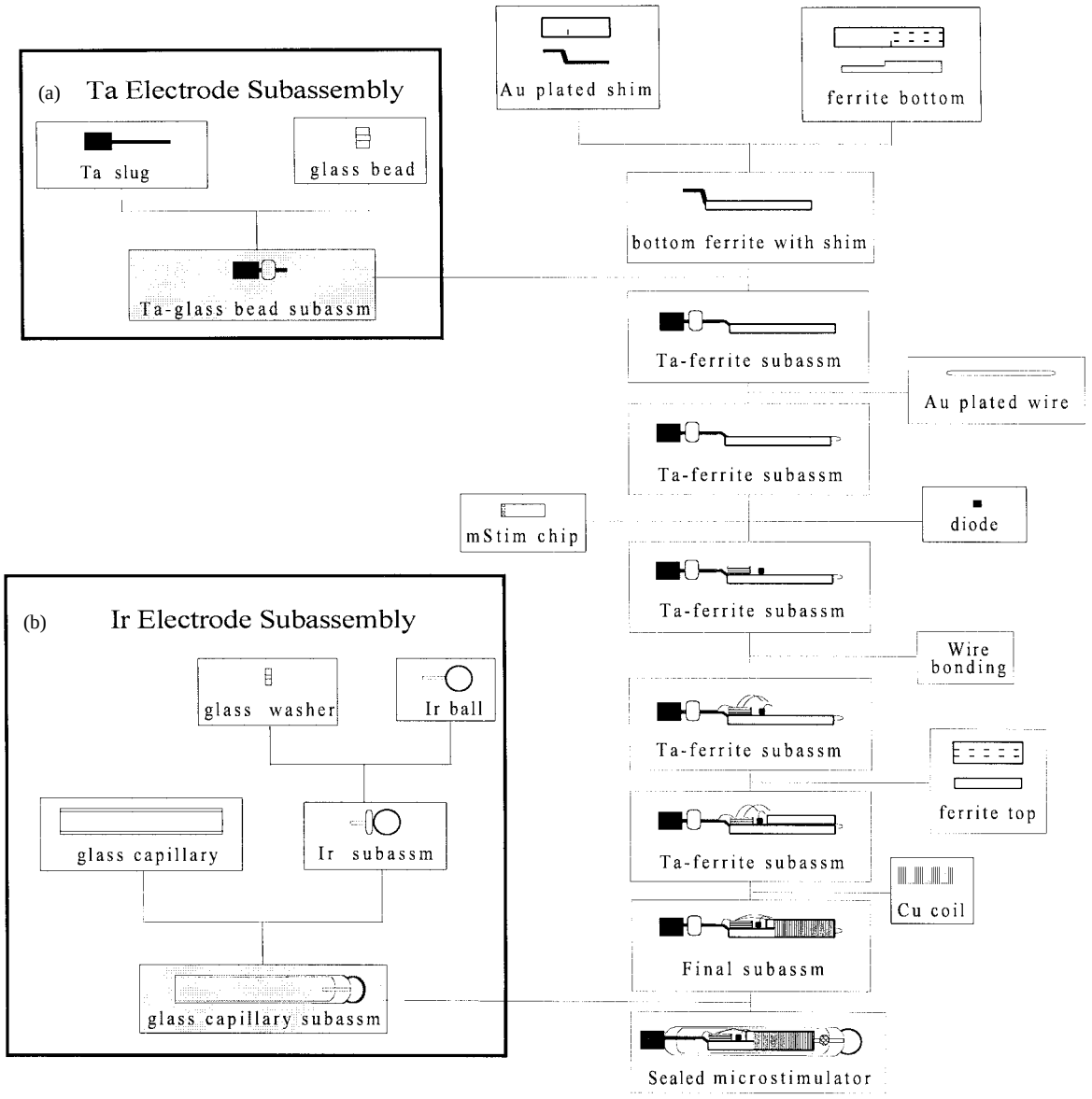

Fig. 3. Schematic diagram of the microstimulator fabrication sequence showing the various steps involved in assembly. (a) The Ta and (b) the Ir ends are made separately with all the internal components being attached at the Ta end first. The final step involves inserting the Ta end and all the various components into the Ir end, which contains the glass capillary tube used as the encapsulating material. Electrochemical conditioning of the two electrodes takes place after the device has been assembled.

are used to compute tensile stress in pounds per square inch (lb/in^2) in these regions as shown in the equation in Fig. 2. After examination of the various seals it was determined that stresses were being created by an uneven distribution of heat during seal formation which was exaggerated by the use of heat sinks. Mockups fabricated by rotating the device at 78 rpm and removing all heat sinks, with the exception of the Ta heat sink, exhibited the least amount of stress and most uniform annealing. The Ta heat sink acts to protect the Ta slug from possible ignition during sealing as well as holds the device in place. The stresses in these samples were consistently under 2000 lb/in^2 (140 kg/cm^2), with compressions observed to be evenly distributed on the metal feedthroughs as desired to maintain hermeticity. Thus all subsequent devices were sealed under these conditions.

6) Fabrication Sequence: The microstimulator is fabricated in three main steps. The first step involves preparing the electrodes. A glass bead is melted to the Ta stem [Fig. 3(a)]; a glass washer is melted to the Ir stem [Fig. 3(b)] and then to the glass capillary tube. This is necessary to protect the IC chip from heat during the glass-to-metal sealing process, whereas, the lesser heat (approximately 80 °C at 2 mm from where the heat is being applied) conducted during the glass-to-glass sealing is safe for the chip. The second step involves assembling the various internal components (listed in Table II) and attaching them to the Ta-glass bead end. The final step involves inserting the electronic subassembly into the Ir-glass capillary section and making a final hermetic seal at the Ta-glass bead to glass capillary junction. The three steps are described in more detail below.

The Ta stem is first polished (by hand using a miniature rotary polishing tool and a polishing paste containing diamond dust) to remove any longitudinal grooves formed during the drawing of the wire by the manufacturer. Such features interfere with the ability to achieve a completely hermetic seal. The stem is then cleaned in petroleum ether, followed by alcohol, and finally distilled water. The Ta slug is then inserted into a Ta heat sink/holder and a microtorch is used to melt a glass bead onto the Ta stem. Ta is used for the holder in order to reduce possible contamination of the electrode by foreign metals, which would interfere with later anodization. The microtorch uses a pressurized natural gas and oxygen flame and the torch tip utilizes a 22-gauge blunt-tip disposable needle (Glenmark Manufacturing Inc., Vernon Hills, IL). The end of the stem opposite the Ta slug is ground flat and cut to length, providing a surface for spot-welding in a later step [Fig. 3(a)]. The Ir electrodes are manufactured by melting a piece of iridium wire 0.010 in in diameter to form a ball approximately 0.065 in in diameter. A glass washer is then melted onto the stem and back side of the ball and the stem cut to length [Fig. 3(b)]. The Ir ball-glass washer subassembly is heat-sealed to the glass capillary and the capillary is cut to length. The Ir ball on the Ir-capillary subassembly is polished and cleaned, as described for the Ta stem, and put aside to be used at a later step.

The main objective in the assembly of the internal components is to mechanically connect the two electrodes and the copper coil to the integrated circuit (IC) chip. This begins by using a two part epoxy resin (J-B Weld, J-B Weld Company, Sulphur Springs, TX) to glue a gold-plated shim to the bottom half of the ferrite core. The shim serves as a platform for the IC chip and diode. The Ta-glass bead subassembly is then spot welded (20 Ws) to the shim. A gold-plated wire feed-through is glued into the groove of the ferrite bottom, for later use as a contact between the IC chip and the Ir ball electrode. Next, the IC chip and diode are attached to the shim with J-B Weld epoxy, and connections between the electrodes and chip are made using a wire ball-bonder on the chip surface and conductive silver-epoxy (H20E, Epoxy technology Inc., Billerica, MA) on the shim and feed-through surface. Hanging gold wires are then bonded to the IC chip to provide a means to connect the coil wires. The ferrite top is bonded to the ferrite bottom with cyano-acrylate adhesive and the copper coil is wound around the entire core. The self-resonance frequency of the coil is adjusted to 2 MHz ($\pm$0.02) by changing the number of turns, while monitoring the resonance with a free-standing grid-dip meter and sweep oscillator. Next, the free ends of the coil leads are stripped of their insulation and attached to the hanging gold wires with conductive epoxy.

In the final step, conductive epoxy is inserted into the Ir-glass capillary subassembly to provide an electrical connection between the Ir ball and the IC chip (via the gold-plated feedthrough wire inside the ferrite core). The electronic subassembly is then sealed into the Ir-glass capillary subassembly.

7) Power Transmission: Magnetic inductive coupling is used to transfer power and data to the implanted devices [39]. The main problem with this type of transmission is that it relies on an airgap transformer that has a very low coupling coefficient between the primary and secondary windings. The flux density outside the primary coil drops precipitously for distances greater than the radius of the coil; this limits the useful range over which the implanted devices can be powered and also reduces electromagnetic emissions to levels acceptable for regulatory authorities. A carrier at 2 MHz was chosen for this application because it lies between the AM and FM radio bands, it can be easily divided into a 1-μs clock needed for pulse-width control, it can be handled efficiently by CMOS circuitry, and it allows sufficient Q to be obtained between the transmitting coil and the small self-tuned receiver coil. Details of the class E driver used to obtain efficient power transmission from the external controller to the implanted microstimulator are described elsewhere [40], [41]. We have made transmission coils ranging from 9-cm diameter $\times$ 1-cm height to 20-cm diameter $\times$ 37-cm length. These have required 1–6 W of power to operate.

8) Data Encoding: A single stimulus pulse from a single microstimulator is specified by three 8-b command words [33]. A 2-MHz carrier is amplitude modulated to transmit this information. Manchester encoding was used because it requires at least one state change every bit, thereby insuring a constant load to the transmitter. A zero is encoded by maintaining state during the 16 carrier cycles comprising 1 b (8 μs), and a one is encoded by a state change after the eighth cycle. A low state is 80% of the high state in carrier amplitude. A complete transmission requires 288 μs, enabling a possible 69 separate devices to be activated sequentially at the maximum specified rate of 50 output pulses/s for each device. During the idle period between commands, alternating zeros and ones are transmitted to all implanted devices. The beginning of a command is signaled by transmitting a ready code made up of five 0 bits. This code is followed by three command words which code for the device address, pulse width, and waveform.

The IC chip in each microstimulator contains an 8-b address stored in read-only-memory, which it compares to the address sent by the controller. If a match is found, the remaining two command words are decoded to determine the pulse width, current, recharge rate, and shape. The second 8-b word decodes the pulse width, which varies from 3–258 μs in 1-μs steps (a minimum of 3 μs occurs due to the finite time needed to switch the circuitry). The final 8-b word determines the rest of the stimulus parameters. The four high bits (C_7–C_4) are used for the stimulus current amplitude, providing 16 levels. Bit 3 determines the current range, low (0–3 mA, 0.2 mA steps) or high (0–30 mA, 2 mA steps). Bit 2 determines the pulse shape, which can be square or have a tail that drops exponentially by adding a holdup capacitor on the input to the stimulus current control circuit. A stimulus waveform that has an exponential tail can be used with certain nerve cuff electrode configurations to preferentially stimulate small diameter motor axons while anodally blocking large axons [42]. Bit 1 selects the recharge current (20 or 200 μA), and bit 0 is used to maintain even parity, which is used as one of the data integrity checks. An additional check consists of the mandatory data $= 1$ bits that occur every fifth bit; these also assure that the five sequential zeros used as the ready code are unique.

9) External Control: Control of the transmitter was accomplished by a Motorola 68HC11 microcontroller connected to

an Actel A1020 series field programmable gate array (FPGA) [43]. This architecture was chosen for its flexibility and small size. The Motorola 68HC11 contains the required ports and ample memory on a single chip requiring little external circuitry. The microprocessor was programmed as a stand-alone device to deliver stored stimulation sequences at regular intervals. During the chronic animal experiments, information on up to four cats was programmed into the internal memory nonvolatile and used to produce the desired stimulation sequences for the training sessions. A second program provided real-time control of the pulse width and amplitude according to dials on the front panel of the control box. Both modes controlled up to four implants independently. When instructed, the three 8-b control words were sent sequentially to an 8-b parallel port on the FPGA. The FPGA performed a parallel to serial conversion, adding the various additional bits required by the transmission protocol and the Manchester encoding needed by the carrier modulating circuitry. The digital circuitry was implemented on an FPGA in order to reduce the physical size of the control unit while maintaining flexibility during the design and testing phase.

B. In Vitro Testing

In vitro testing was performed to assess the functionality of the sealed microstimulators before their implantation into muscle. First, the output characteristics (stimulus amplitude and pulse duration) were measured. Each device was placed in a separate saline-filled well (20 mm $\times$ 4 mm $\times$ 6 mm) containing two noncontacting pickup electrodes. The stimulus current generated potential gradients in the saline bath that were recorded differentially by the recording electrodes. This signal was then displayed on an oscilloscope screen and measured.

Second, precise and accurate measurements of stimulus and recharge currents and compliance voltages were made by using a second test bath. This test bath is analogous to the sucrose-gap technique used to monitor the action currents produced by an axon, which involves forcing the currents through an external path whose electrical resistance can be controlled.

Third, each device was tested for its ability to couple with the external coil. Devices were placed inside the external coil and rotated through 180°; the resulting stimulus pulse was displayed on an oscilloscope screen and measured.

C. In Vivo Testing

We examined the effects of the body environment on the function of the microstimulators by implanting a total of 12 devices through a 12-gauge angiocath into the hind limb muscles of three cats. To insert the tested devices two skin incisions were made in each limb. One incision extended along the anterior surface of the shank, and the other along the posterior surface from the popliteal fossa to the calcaneum. This exposed the muscles to be implanted and allowed us to suture the muscle at the muscle insertion point. These devices were activated 2 h daily, five days a week for a period of up to three months [43]. Devices were examined for any changes on the exposed surface before and after implantation by dissecting microscope and environmental scanning electron microscope (ESEM; model E-3, Electroscan). The condition of the anodization layer of the Ta electrode was assessed before and after implantation by comparing leakage current versus applied voltage recorded before and after implantation. We monitored electrode placement within the muscle by tying a small suture in the muscle next to the iridium end of the device. The location of this suture with respect to the device was examined when the device was removed. The effects of the implants on the tissue will be described in a separate article in preparation.

III. Results

A. In Vitro Testing

Output currents were found to be linear over the low and high current range, up to the compliance voltage limit of the device in the bath (see Fig. 4 and legend). The impedance of the bath was calculated to be 500 Ω and a compliance voltage of approximately 8.8 V was calculated. The two recharge current rates were measured to be 20 μA and 200 μA, respectively. A measurement of the output voltage when the devices were commanded to produce maximum currents (30 mA) with maximum duration pulses (258 μs), and varying interval rate is shown in Fig. 5. As the rate was increased above the interval needed to fully recharge the capacitor electrode, a steady decline in output signal occurred. The 3-dB cutoff frequency was found to be 15 Hz at the 20-μA recharge rate and 120 Hz for the 200-μA recharge rate. The mean angular deviation from the center line up to the limit where the microstimulator functioned normally was found to be $\pm 55.5 \pm 6.4^{\circ}$ ($n = 10$).

We were able to isolate three different failure modes of the devices. The first failure mode was the development of gross leaks. These leaks resulted in visible water condensation on the glass walls within a few hours to a few days of *in vitro* testing. They were associated with visible cracks in the seals, due to stresses in the glass. The incidence of such cracks was reduced after the changes in sealing procedure described above, but the yield of functioning devices remained low (about 40%) because of poor control of heating during the sealing process.

A second failure mode involved the condensation of entrapped water vapor. The microtorch sealing method and the various hygroscopic internal components made it impossible to eliminate water vapor trapped within a hermetically sealed package. This entrapped water vapor can cause detuning of the coil and subsequent intermittent behavior.

A third failure mode occurred when output connections broke. The conductive silver-epoxy which connects the electronic components to the iridium electrode stem tended to become brittle with age. It has also been found to produce undesirable volatiles. Some failures of this electrical connection were detected during the dc leakage test, which required passage of current from a probe on the external iridium ball though the electronics and out the tantalum electrode into a saline bath.

Only those device that passed *in vitro* testing were implanted into animals.

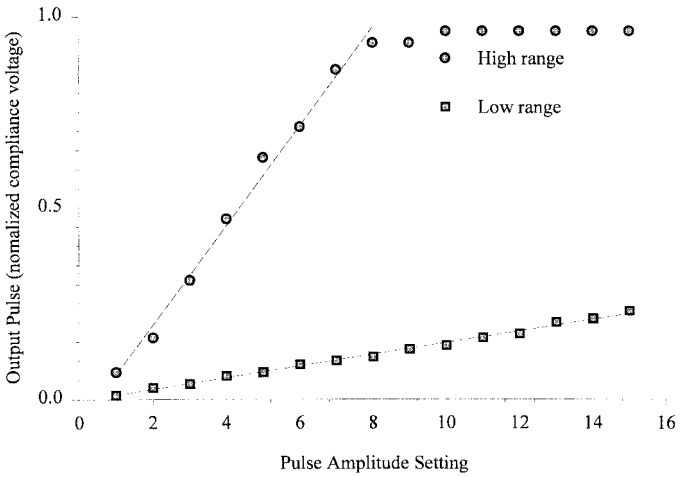

Fig. 4. Graph of pulse amplitude setting versus normalized output voltage. The linear portion of the curves were fitted to straight lines which are displayed on the graph as dashed lines. These lines were found to fit very closely to the data with standard error of estimate (Sy.x) values of 7.0×10^{-3} and 3.1×10^{-2} for the low and high current ranges, respectively.

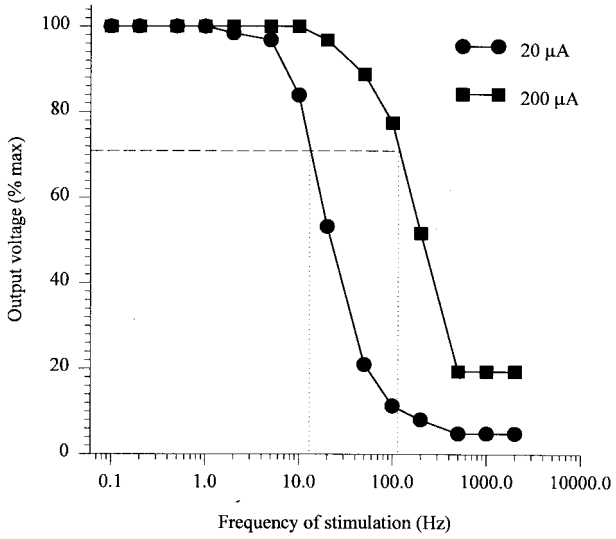

Fig. 5. Graph of the frequency of stimulation versus the output voltage as a percentage of maximum voltage for the two recharge currents. The 3-dB cutoff frequencies at the two rates are shown by the dotted lines, 15 and 120 pulse per second (pps) for 20 μA and 200 μA, respectively. Devices were commanded to produce maximum currents and pulse widths throughout this test. Actual currents were limited by compliance voltage to approximately 16 mA.

B. In Vivo Testing

Muscle tissue and chronic stimulation was not found to cause any changes in the surface of the microstimulators. Of the 12 implanted devices all but one functioned normally at the end of the experiment. The device that stopped functioning was found to contain water vapor, which had entered through small cracks in the glass seal at the Ta end. This crack was thought to have developed over time because of residual stress in the glass after sealing. None of the devices were found to migrate; at explantation all devices were found next to the suture that was tied at the time of implantation [44].

Post-implant ESEM views of both electrode surfaces and the glass capsule showed no detectable changes from nonimplanted devices except for a dense coating of connective tissue on the corners of the tantalum slug (Fig. 6).

Leakage currents were measured before and after implantation. Curves from one device are shown in Fig. 7. At a nominal operating level of +10 VDC, leakage currents were measured as 6 μA (pre-op) and 1 μA (post-explant). This improvement may have resulted from slow completion of the anodization of the deepest parts of the sintered surface as a result of biasing by the recharge power supply. Post-implant dc capacitance was estimated to be 2.7 μF, which is consistent with the value expected for the thickness of the anodization layer.

IV. Discussion

The electrical properties of the microstimulators described in this report are within specifications and suitable for a wide range of clinical applications. Some improvement is desirable, however, in the present approach to packaging. It was difficult to control adequately the heating from the microtorch, which resulted in residual stress in the glass capsule. Low yields resulted due to blowouts of the molten glass caused by expansion of air in the capsule. Residual moisture produced by the flame and trapped in the capsule is also a concern. The rigid mechanical and electrical connection between the electronic subassembly and the iridium electrode by conductive epoxy is undesirable, particularly if the device is to be temperature cycled during testing on sterilization. We are working on a new strategy in which an infrared laser is used to produce all of the glass seals. The feed-through at the Ir electrode end will consist of a hollow tube plus a spring that contacts the electronic subassembly. After the glass sealing is completed, the device can be baked out and back-filled with inert gas prior to closing off the tube and attaching a washer-shaped Ir electrode using a conventional yttrium aluminum garnet (YAG) production laser. These changes are expected to eliminate the failures seen in the present study.

The flexibility of these microstimulators make them ideal for many FNS application. Multiple single-channel devices can be injected into various muscles or regions of a single muscle allowing for a more precise control of movement without the need for multiple leads and controllers. Control of the microstimulator can be achieved in any combination of channels from 1–256 through a single externally worn coil. Eight channel stimulators have been described [45]–[47] with some recent work being done on 30- and 64-channel systems [48].

The small size of the microstimulators allows them to be easily implanted into locations that may be difficult to reach using standard surgical techniques and electrodes requiring connecting leads. We have developed an insertion tool made from a 12-gauge angiocatheter that can be used to test stimulation locations by passing electrical current through the tip of the needle before the injection of the permanently implanted devices. Some of the applications of FNS that may be suited for this type of technology include urinary control, bowel management, sexual function, pain management, as well as the control of manipulation and mobility. Like most FNS devices, microstimulators activate muscle fibers indirectly by

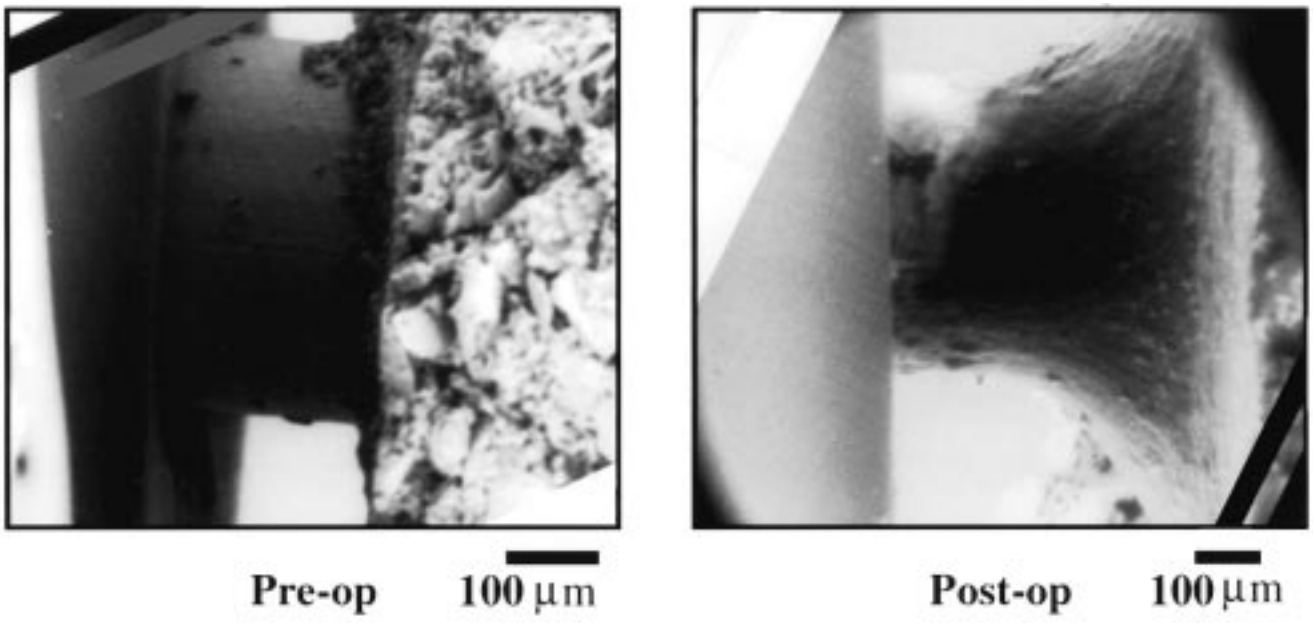

(a) (b)

Fig. 6. Photograph of environmental scanning electron micrographs of the Ta stem and slug before (pre-op) and after (post-op) implantation. A layer of connective tissue is seen around the stem of the post-op device.

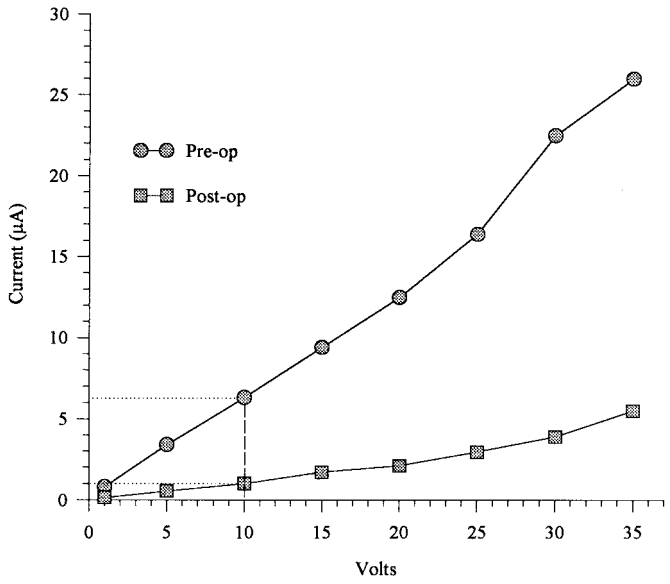

Fig. 7. Graph of the applied voltage versus the measured leakage current for devices before and after chronic implantation into the muscle of a cat. The dotted lines indicate the leakage current measured at the normal operating voltage of 10 V.

exciting the terminal branches of motoneurons, so they are most appropriate for paralysis and paresis caused by upper motor lesions in which the motoneurons and peripheral nerves remain intact.

Microstimulators can also be used in muscles located too deep for surface stimulation. Other applications include post-operative therapy following hip or knee surgery. A lack of mobility in these patients can greatly increase their rehabilitation time; by maintaining muscle strength, recovery time could be reduced. Microstimulators are ideal solutions for these types of therapeutic applications because they are easily implanted nonsurgically and do not need to be removed after the rehabilitation period, because they are essentially inert when not actively powered. However, in the event of an infection they could be removed surgically. The transmitter power required for continuous operation of our present implant is probably too high for most portable FNS applications, so initial use will most likely be for TES at the bedside or while seated. The next generation devices that incorporate the new packaging approaches will also use a much more efficient power and data transmission scheme that should enable portable applications.

V. Conclusions

A single-channel injectable electrical stimulator was designed, fabricated, and tested. The implanted devices were found to maintain hermeticity in most cases for the duration of the test period (three months) and were able to produce highly controllable stimulation pulses capable of causing reproducible twitches when applied to various muscles of a cat. This device has many advantages over previous devices. First, it is completely self-contained, which eliminates the need for internal cables and wires that are susceptible to mechanical failure and infection. The modularity of the device enables it to be easily configured into a custom multichannel system. The use of capacitor electrodes reduces the possibility of net direct current flow in the event of failure in the control electronics. Anodized Ta has a very low leakage current which was found to be stable or even decrease with chronic stimulation. Finally, its small size allows implantation with minimal surgery. Biocompatibility and recruitment characteristics of these devices are presently under study.

ACKNOWLEDGMENT

The authors would like to thank J. Conway for assistance in the preparation of the manuscript.

REFERENCES

[1] R. M. Glaser, "Functional neuromuscular stimulation exercise conditioning of spinal cord injured patients," *Int. J. Sports Med.*, vol. 15, pp. 142–148, 1994.

[2] R. D. Malagodi, M. W. Ferguson-Pell, and R. D. Masiello, "A functional electrical stimulation exercise system designed to increase bone density in spinal cord injured individuals," *IEEE Trans. Rehab. Eng.*, vol. 1, pp. 213–219, 1993.

[3] I. Arvidsson, "Prevention of quadriceps wasting after immobilization: An evaluation of the effect of electrical stimulation," *Orthoped.*, vol. 9, p. 1519, 1986.

[4] R. W. Fields, "Electromyographically triggered electric muscle stimulation for chronic hemiplegia," *Arch. Phys. Med. Rehabil.*, vol. 68, pp. 407–413, 1983.

[5] R. S. Gotlin, S. Hershkowitz, P. M. Juris, E. G. Gonzalez, N. Scott, and J. N. Insall, "Electrical stimulation effect on extensor lag and length of hospital stay after total knee arthroplasty," *Arch. Phys. Med. Rehab.*, vol. 75, pp. 957–959, 1994.

[6] M. W. Keith, P. H. Pechham, G. B. Thorpe, K. C. Stroh, B. Smith, J. R. Buckett, K. L. Kilgore, and J. W. Jatch, "Implantable functional neuromuscular stimulation in the tetraplegic hand," *J. Hand Surg.*, vol. 14, pp. 524–530, May 1989.

[7] Y. Handa, T. Handa, Y. Nakatsuchi, Y. Tagi, and N. Hoshimiya, "A voice-controlled functional electrical stimulation system for the paralyzed hand," *Iyodenshi to Seitai Kogaku*, vol. 23, pp. 292–298, 1985.

[8] D. Rudel, T. Bajd, A. Kralj, and H. Benko, "Surface functional electrical stimulation of the hand in quadriplegics," in *Proc. 5th Annu. Conf. Rehab. Eng.*, 1982, p. 59.

[9] A. Prochazaka, M. Gauthier, M. Wieler, and Z. Kenwell, "The bionic glove: An electrical stimulator garment that provides controlled grasp and hand opening in quadriplegia," *Achc. Phys. Med. Rehab*, to be published.

[10] J. K. Klose, B. Needham-Shropshire, N. H. Lubwohl, and B. A. Green, "The results of a 35 SCI subject experience with the parastep-1 walking system," *J. Amer. Paraplegia Soc.*, vol. 17, p. 115, Apr. 1994.

[11] E. B. Marsolais and R. Kobetic, "Functional walking in paralyzed patients by means of electrical stimulation," *Clin. Orthoped. Rel. Res.*, vol. 175, pp. 30–36, May 1983.

[12] B. J. Andrews, R. H. Baxendale, R. Barnett, G. F. Phillips, T. Yamazaki, J. P. Paul, and P. A. Freeman, "Hybrid FES orthosis incorporating closed loop control and sensory feedback," *J. Biomed. Eng.*, vol. 10, pp. 189–195, Apr. 1987.

[13] D. Popovic, R. Tomovic, and L. Schwirlich, "Hybrid assistive system—Neuroprosthesis for motion," *IEEE Trans. Biomed. Eng.*, vol. 36, pp. 729–738, 1989.

[14] M. R. Solomonow, R. Barratta, D. Shoji, N. D'Ambrosia, W. Rightar, R. Walker, and R. Beandette, "FES powered reciprocating gait orthosis for paraplegic locomotion," in *Proc. Vienna Int. Workshop on Electrical Stimulation*, 1983, p. 81.

[15] W. W. L. Glenn and M. L. Phelps, "Diaphragm pacing by electrical stimulation of the phrenic nerve," *Neurosurg.*, vol. 17, pp. 974–984, 1985.

[16] A. F. Dimarco, W. Kovvuri, J. Petro, and G. Supinski, "Intercostal muscle pacing in venatitor-dependent quadriplegics," *Amer. Rev. Respirat. Dis.*, vol. 143, p. A473, 1991.

[17] G. S. Brindley, C. E. Polkey, D. N. Rushton, and L. Cardozo, "Sacral anterior root stimulators for bladder control in paraplegia: The first 50 cases," *J. Neurol. Neurosurg. Psych.*, vol. 49, pp. 1104–1114, 1986.

[18] G. S. Brindley and D. N. Rushton, "Long-term follow-up of patients with sacral anterior root stimulator implants," *Paraplegia*, vol. 28, pp. 469–475, 1990.

[19] N. R. Binnie, A. N. Smith, G. H. Creasey, and P. Edmond, "Constipation associated with chronic spinal cord injury: The effect of pelvic parasympathetic stimulation by the Brindley stimulator," *Paraplegia*, vol. 29, pp. 463–469, Sept. 1991.

[20] A. S. Haleem, F. Boehm, A. D. Legatt, A. Kantrowitz, B. Stone, and A. Melman, "Sacral root stimulation for controlled micturition: Prevention of detrusor-external sphincter dyssynergia by intraoperative identification and selective section of sacral nerve branches," *J. Urol.*, vol. 149, pp. 1607–1612, June 1993.

[21] A. Stefanovska, S. Rebersek, T. Bajd, and L. Vodovnik, "Effects of electrical stimulation on spasticity," *Crit. Rev. Phys. Rehab. Med.*, vol. 31, pp. 59–99, 1991.

[22] C. J. Robinson, N. A. Kett, and J. M. Bolam, "Spasticity in spinal cord injured patients: 2. Initial measures and long-term effects of surface electrical stimulation," *Arch. Phys. Med. Rehab.*, vol. 69, pp. 862–868, 1988.

[23] P. E. Crago, P. H. Peckham, J. T. Mortimer, and J. P. Van Der Meullin, "The choice of pulse duration for chronic electrical stimulation via surface, nerve and intramuscular electrodes," *Ann. Biomed. Eng.*, vol. 2, pp. 252–264, 1974.

[24] J. M. Campbell and P. M. Meadows, "Therapeutic FES: From rehabilitation to neural prosthetics," *Assist. Technol.*, vol. 4, pp. 4–18, 1992.

[25] E. B. Marsolais and R. Kobetic, "Implantation techniques and experience with percutaneous intramuscular electrodes in the lower extremity," *Rehab. Res. Dev.*, vol. 23, pp. 1–8, 1986.

[26] P. H. Peckham, M. W. Keith, and A. A. Freehafer, "Restoration of functional control by electrical stimulation in the upper extremity of the quadriplegic patient," *J. Bone Joint Surg.*, vol. 70, pp. 144–148, 1988.

[27] G. M. Yarkony, E. J. Roth, G. R. Cybulski, and R. J. Jaeger, "Neuromuscular stimulation in spinal cord injury II: Prevention of secondary complications," *Arch. Phys. Med. Rehab.*, vol. 73, pp. 195–200, Feb. 1992.

[28] J. B. Myklebust, Ed., *Neural Stimulation*, vol. 2. Boca Raton, FL: CRC, 1985.

[29] L. L Baker, B. R. Bowman, and D. R. MeNeal, "Effects of waveform on comfort during neuromuscular electrical stimulation," *Clin. Orthoped.*, vol. 233, pp. 75–85, 1988.

[30] M. T. Balmaseda, Jr., M. T. Fatehi, S. H. Koozekanani, and J. S. Sheppard, "Burns in functional electrical stimulation: Two case report," *Arch. Phys. Med. Rehab.*, vol. 68, pp. 452–452, 1987.

[31] R. L. Waters, D. R. McNeal, and J. Perry, "Experimental correction of footdrop by electrical stimulation of the peroneal nerve," *J. Bone Joint Surg.*, vol. 57, pp. 1047–1054, Dec. 1975.

[32] P. Strojnik, R. Acimovic, E. Vavken, V. Simic, and U. Stanic, "Treatment of drop foot using and implantable peroneal underknee stimulator," *Scand. J. Rehab. Med.*, vol. 19, pp. 37–43, 1987.

[33] G. E. Loeb, C. J. Zamin, J. H. Schulman, and P. R. Troyk, "Injectable microstimulator for functional electrical stimulation," *Med. Biol. Eng., Comput.*, vol. 29, pp. 13–19, Nov. 1991.

[34] D. L. Guyton and F. T. Hambrecht, "Theory and design of capacitor electrodes for chronic stimulation," *Med. Biol. Eng., Comput.*, vol. 12, pp. 613–619, 1974.

[35] L. S. Robblee, J. L. Lefko, and S. B. Brummer, "Activated Ir: An electrode suitable for reversible charge injection in saline solution," *J. Electrochem. Soc.*, vol. 130, pp. 731–733, 1983.

[36] D. A. J. Rand and J. Turner, "Cyclic voltammetric studies on iridium electrodes in sulfuric acid solutions. Nature of oxygen layer and metal dissolution," *Electroanal. Chem. Interfac. Electrochem.*, vol. 55, pp. 375–381, 1974.

[37] E. Gruys, J. M. Schakenraad, L. K. Kruit, and J. M. Bolscher, "Biocompatibility of glass-encapsulated electronic chips (transponders) used for the identification of pigs," *Veterinary Rec.*, vol. 133, pp. 385–388, Oct. 1993.

[38] "Standard method for analyzing stress in glass," in *Annual Book of ASTM*. Philadelphia, PA: Amer. Soc. Testing and Materials, 1978.

[39] W. J. Heetderks, "RF powering of millimeter- and submillimeter-sized neural prosthetic implants," *IEEE Trans. Biomed. Eng.*, vol. 35, pp. 323–327, 1988.

[40] P. R. Troyk and M. A. Schwan, "Class E driver for transcutaneous power and data link for implanted electronic devices," *Med. Biol. Eng., Comput.*, vol. 30, pp. 69–75, Jan. 1992.

[41] ———, "Closed-loop class E transcutaneous power and data link for microimplants," *IEEE Trans. Biomed. Eng.*, vol. 39, pp. 589–599, June 1992.

[42] Z. P. Fang and J. T. Mortimer, "Alternate excitation of large and small axons with different stimulation waveforms: an application to muscle activation," *Med. Biol. Eng., Comput.*, vol. 29, pp. 543–547, Sept. 1991.

[43] T. Cameron, G. E. Loeb, F. J. R. Richmond, R. A. Peck, J. H. Schulman, P. Strojnik, and P. Troyk, "Micromodular electronic devices to activate paralyzed muscles and limbs" in *Proc. IEEE EMBS*, 1993, vol. 15, pp. 1242–1243.

[44] T. L. Fitzpatrick, T. L. Liinaamaa, I. E. Brown, T. Cameron, and F. J. R. Richmond, "A novel method to identify migration of small implantable devices," *J. Long-Term Effects Med. Implants*, to be published.

[45] J. R. Buckett, P. H. Peckham, G. B. Thrope, S. D. Braswell, and M. W. Keith, "A flexible, portable system for neuromuscular stimulation

in the paralyzed upper extremity," *IEEE Trans. Biomed. Eng.*, vol. 35, pp. 897–904, Nov. 1988.
[46] P. Strojnik, P. Meadows, J. H. Schulman, and D. Whitmoyer, "Modification of a cochlear stimulation system for FES applications," *Basic Appl. Myol.* vol. 4, pp. 129–140, 1994.
[47] N. Donaldson, "A new multiplexed stimulator for FNS," in *Advances in External Control of Human Extremities X*. Belgrade: Yugoslav Committee for ETAN, 1987, pp. 41–50.
[48] Y. Handa, T. Handa, M. Ichie, H. Murakami, N. Hosimiya, S. Ishikawa, and K. Ohkubo, "Functional electrical stimulation (FES) systems for restoration of motor function of paralyzed muscles—Versatile systems and a portable system," *Frontiers Med. Biol. Eng.*, vol. 4, pp. 241–255, 1992.

Tracy Cameron (S'93–M'96) was born in Oshawa, Canada, in 1962. She received the B.Sc. degree in biochemistry from Queen's University, Kingston, Ont., Canada, in 1985, the M.S. degree in biomedical engineering from the University of Miami, Coral Gable, FL, in 1988, and the Ph.D. degree in physiology from Queen's University, Kingston, in 1996.

In 1988, she worked as a Biomedical Engineer at The Miami Project to Cure Paralysis, University of Miami. There she became interested in the application of neural prosthetics to restore movement. She continued this interest during her study towards the Ph.D. degree, when she was involved in the development and testing of miniature implantable stimulators. She is currently examining the application of neural prosthetics, in both the suppression of tremor and in hand opening of paretic limbs, as a Post-Doctoral Fellow at the Division of Neuroscience, University of Alberta, Alta, Canada.

Gerald E. Loeb was born in New Jersey in 1948. He received the B.A. and M.D. degrees from the Johns Hopkins University, Baltimore, MD, in 1969 and 1972, respectively.

After a year of clinical training in surgery at the University of Arizona, Tucson, he joined the Laboratory of Neural Control at the National Institutes of Health, Bethesda, MD, as a Commissioned Officer in the Public Health Service. In his 15 years there, he worked on basic sensorimotor neurophysiology and developed many implantable transducers and electrodes for studies in unrestrained animals; more recently, this work has been extended to model-based analysis of musculoskeletal mechanics and neural control. Since 1969, he has been actively involved in clinical applications of neural prosthetic technology to restore vision (at the University of Utah, Salt Lake City), hearing (at University of California at San Francisco) and neuromuscular control (with the A. E. Mann Foundation). He consults widely in the medical device industry and has written more than 100 journal articles, ten patents and a textbook on electromyography. He has been at Queen's University in Kingston, Ont., Canada, since 1988, now as Director of Bio-Medical Engineering and Professor of Physiology, and serves in an advisory role as Chief Scientist of Advanced Bionics Corp., Sylmar, CA.

Raymond A. Peck was born in Ipswich, England, in 1946 and educated at both St. Lawrence College and Queens University, Kingston, Ont. Canada.

His interests in commerce, fine art, and science led initially to painting and sculpture and a position of Manager for the department of a large graphics company in Toronto, Ont. He started his own business manufacturing jewelry involving electroplating, anodizing, injection molding, and fine sculpture. In 1990, he took a position with the Bio-Medical Engineering Unit, Queen's University, specializing in Microfabrication. The majority of this work has been with the fabrication of the microstimulator and manufacturing prototypes of cochlear implants and other implantable electrodes.

Joseph H. Schulmau (S'57–M'67–LM'97) received the B.S. degree in applied physics in 1960 and the Ph.D. degree in zoology in 1969 with specializations in spectroscopy, genetics, and neurophysiology from the University of California at Los Angeles (UCLA).

He worked in electronics design and sensory physiology at North American Aviation, Downey, CA, Litton Industries, Beverly Hills, CA, and Bell Labs, Murray Hill, NJ. In 1969, he was the Technical Founder of Pacesetter Systems (now the second largest cardiac pacemaker company in the world). He managed and designed the CLARION cochlear program leading to the founding of Advanced Bionics. Neurodyne Corporation, Alfred E. Mann Foundation, MiniMed, and Siemens Infusion were additional outgrowths from the original Pacesetter organization. For 27 years, he has been Director, Chief Scientist, Vice President of R&D, and President of companies arising from Pacesetter. Among his achievements are rechargeable cardiac pacemaker (more than 1000 implanted for 20 plus years), first two-way telemetry in pacemakers, intracranial pressure monitor, dual channel programmable rechargeable neural stimulator, simulator to test cardiac pacemakers, multichannel portable computerized IV pump, cerebellar stimulator, and the CLARION. He was involved in the development of implantable pumps, advanced cardiac pacemakers, and chemical sensors. Today, he is Director and Chief Scientist at the Alfred E. Mann Foundation, Sylmar, CA, managing sensor, microstimulator, FES, advanced Cochlear implants, and other projects.

Dr. Schulman is a member of Sigma Pi Sigma, Sigma Xi, AlP, ACC, and ARRL.

Primoz Strojnik, photograph and biography not available at the time of publication.

Philip R. Troyk (M'83–SM'91) received the B.S. degree in electrical engineering from the University of Illinois, Urbana, in 1974 and the M.S. and Ph.D. degrees in bioengineering from the University of Illinois, Chicago, in 1980 and 1983, respectively.

He was on the staff of Northrop Corporation, Rolling Meadows, IL, from 1973 to 1981. In 1983, he joined the faculty of the Illinois Institute of Technology, where he is currently an Associate Professor in the Pritzker Institute of Medical Engineering and the Department of Electrical and Computer Engineering. His interests include the design and packaging of electronic assemblies for implantation in the human body and polymeric protection of thin film devices operating in high-humidity environments.

Dr. Troyk is a member of Phi Kappa Phi and the American Chemical Society.